Nano-structured micro-reactors

Theory: H. Ruhl, J. Bekx, C. Bild, O. Jaura, M. Lienert, J. Niemeyer, M. Nöth, G. Raj, M. Touati, N. Yadev
Experiment: A. Broderson, P. Fischer, E. Gaul, B. Gonzales, J. Hartmann, G. Holzer, S. Kumar, D. Nebe, K. Rani, M. Schollmeier, A. Schuster, V. Scrutelnic, V. Shirvanyan, M. Speicher, S. Steinke, J. Warner

Marvel Fusion GmbH, Munich, Germany
$p^{11}B$ Workshop Catania
Sept 05, 2022

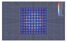

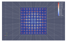

The nano-structured micro-reactor concept

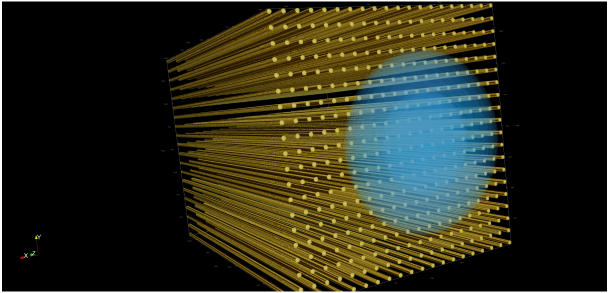

Figure: The target consists of 400 cylindrical boron - proton - deuteron nano-rods, rod radius $R = 100$ nm, rod gap $D = 600$ nm. The laser pluse length is $\tau \approx 30$ fs, laser intensity is relativistic for electrons,the laser wavelength is $\lambda = 400$ nm,the laser spot size is $R_L \approx 4\,\mu$m, and the polarization is circular.

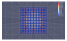

The nano-structured micro-reactor concept

- The reactor concept is microscopic.
- The reactor concept is nano-structured.
- The reactor concept is all fuel based.
- The reactor operates at near solid density.
- Nanoscopic fuel seeding is analyzed.
- Drift fields are analyzed.

- Goal A: Improvement of nuclear fusion over pitcher - catcher configuration.

Nanoscopic seeding

The basic framework is

$$\frac{\partial f_k}{\partial t} + \vec{v}_k \cdot \frac{\partial f_k}{\partial \vec{x}_k} + \frac{q_k}{m_k} \left(\vec{E} + \vec{v}_k \times \vec{B} \right) \cdot \frac{\partial f_k}{\partial \vec{v}_k} = \sum_l \int d^3 v_l \, v_{rel}^{kl} \int d\Omega_\psi \; \sigma_C^{kl} (s, \psi) \left(f_{l'} f_{k'} - f_l f_k \right)$$
$$- \sum_l \int d^3 v_l \, v_{rel}^{kl} \int d\Omega_\psi \; \sigma_R^{kl} (s, \psi) \; f_k \, f_l \, .$$

Nano-acceleration is fast. Hence we have

$$\left(\partial_t + v_k \partial_{r_k} + \frac{e_k}{m_k} E_r \left(r_k \right) \, \partial_{v_k} \right) \left(r_k v_k f_k \right) \left(r_k , v_k , t \right) = 0 \, , \quad r_k \leq R \, , \tag{1}$$

where R is the nano-rod radius and

$$E_r \left(r_k \right) = \begin{cases} C_l \, r_k \, , & 0 \leq r_k < R \\ 0 \, , & r_k \geq R \end{cases} \, , \quad C_l = \frac{e \, n_l}{2 \, \epsilon_0} \, . \tag{2}$$

The solutions are

$$t_k^s = \sqrt{\frac{m_k}{e_k C_l}} \cosh^{-1} \left(\frac{R}{r_k^s(0)} \right) \, , \quad r_k^s(t_k^s) = R \, , \quad g_k^s(t_k^s) = \sqrt{\frac{e_k C_l}{m_k}} \sqrt{R^2 - \left(r_k^s(0) \right)^2} \, . \tag{3}$$

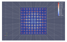

Nanoscopic seeding

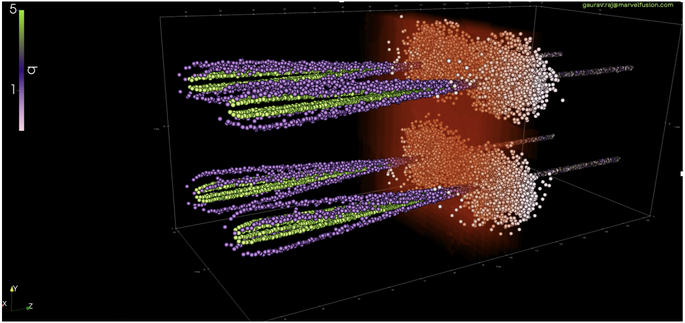

Figure: Short intense laser pulse interacting with nano-rods.

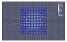

Nanoscopic seeding

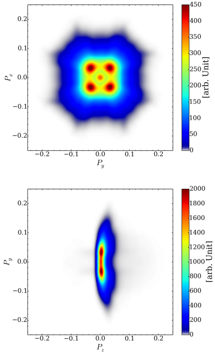

Figure: Proton momentum distributions integrated over the configuration space after the laser pulse has exited the nano-structures. The proton momenta are normalized to $m_\mathrm{p} c$.

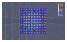

The abstraction model

With the help of the seeding configuration (3) and as outlined in [1] the abstraction model is

$$\frac{dN_k(t)}{dt} \approx -N_k^2(t)\,\frac{N}{V}\,\sum_s \alpha_k^s\, g_k^s(t)\,\sigma_R^{kl}\left(g_k^s(t)\right)\ , \tag{4}$$

where

$$\frac{d\vec{g}_k^{\,s}(t)}{dt} \approx \frac{e_k}{m_k}\left[\vec{E}\left(\vec{r}_k^{\,s}(t),\, t\right) + \vec{g}_k^{\,s}(t)\times\vec{B}\left(\vec{r}_k^{\,s}(t),\, t\right)\right] - \nu_{ke}^s\left(g_k^s(t)\right)\,\vec{g}_k^{\,s}(t) \tag{5}$$

and

$$\frac{d\vec{r}_k^{\,s}(t)}{dt} = \vec{g}_k^{\,s}(t)\ , \tag{6}$$

where N_k is the number of fuel ions of sort k, the $\vec{g}_k^{\,s}$ are the fuel velocities of sort k, the $\vec{r}_k^{\,s}$ are the fuel positions of sort k, the quantities $\vec{E}$ and $\vec{B}$ denote the electromagnetic field context, and the ν_{ke}^s energy draining resistivities given by

$$\nu_{ke}^s\left(\vec{g}_k^{\,s}(t)\right) \approx \frac{e_k^2 e_e^2\, n_l}{4\pi\,\epsilon_0^2 m_{ke}^2\,\left|\vec{g}_k^{\,s}(t) - \vec{v}_e(t)\right|^3}\ \ln\Lambda_{ke}\ , \tag{7}$$

where $\vec{v}_e$ is the electron velocity at the position $\vec{r}_e$ and n_l the fuel density of sort l.

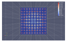

Mixed fuel cross sections

As the (4) implies the conversion efficiency η^{kl} is limited by

$$\eta^{kl} \leq n_l \, \mathcal{R}_k \, \sigma_0^{kl} \,, \quad \mathcal{R}_k \approx \int_0^{t_C} dt \, g_k(t) \,, \tag{8}$$

while the velocity is determined by the initial seeding fields as well as secondary fields. The nuclear fusion cross sections are parametrized as

$$\sigma_R^{kl}\left(\vec{g}_k^{\,s}(t)\right) \geq \begin{cases} \sigma_0^{kl} \,, & \sqrt{\dfrac{2\epsilon_1^{kl}}{m_k}} \leq \left|\vec{g}_k^{\,s}(t)\right| \leq \sqrt{\dfrac{2\epsilon_2^{kl}}{m_k}} \\ 0 \,, & \text{else} \end{cases} \,, \tag{9}$$

where σ_0^{kl}, ϵ_1^{kl}, and ϵ_2^{kl} with $\epsilon_1^{kl} \leq \epsilon_2^{kl}$ are the parameters required to fix a lower limit approximation of the multi cross sections considered. An example is given in Fig. 4.

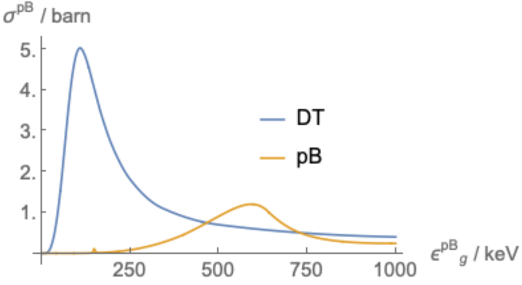

Figure: Comparison between the cross sections of pB and DT as quoted in reference [2].

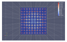

The drift field configuration

Simulations indicate that secondary fields are generated in the nano-structures as well. We make a parametric ansatz for the secular electromagnetic field context

$$\vec{B}\,(\vec{r},\,t) \quad \approx \quad \begin{cases} \dfrac{j_e r}{2\epsilon_0 c^2}\,\vec{e}_\phi\,, & r \leq R_L \\ 0\,, & r > R_L \end{cases} \quad , \tag{10}$$

where $j_e = q_e n_e v_e$ is the strength of the electronic current density. The electric field associated with j_e and B is

$$\vec{E}\,(\vec{r},\,t) \quad \approx \quad \begin{cases} \dfrac{j_e^2\, r}{2\epsilon_0\, c^2\, q_e n_e}\,\vec{e}_r & r \leq R_L \\ 0 & r > R_L \end{cases} \quad , \tag{11}$$

where R_L is the approximate diameter of the electronic forward current.

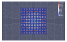

The drift field configuration

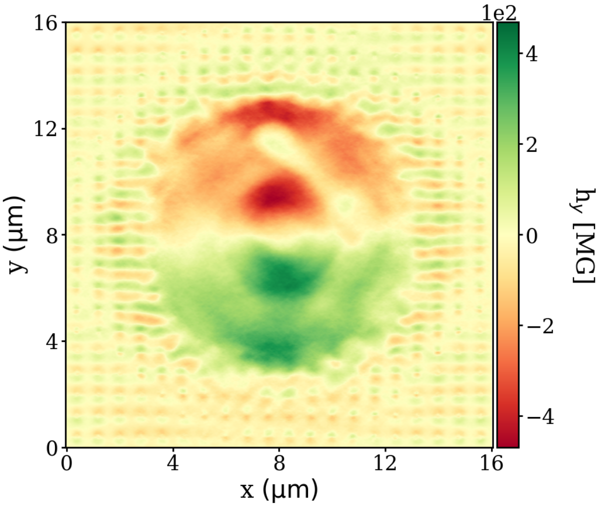

Figure: Simulated magnetic drift field.

The drift field configuration

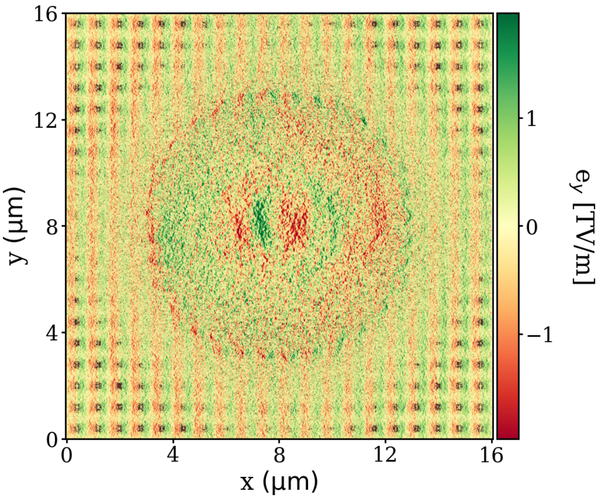

Figure: Simulated electric drift field.

Drift motion of fuel ions

The abstraction model implies

$$\frac{d\vec{x}_k^{\,s}}{dt} = \vec{g}_k^{\,s} \,, \tag{12}$$

$$\frac{dg_{kx}^{s}}{dt} = -\frac{q_k \, \left(E\, x_k^s - g_{kz}^s \, B\, x_k^s \right)}{m_k \sqrt{\left(x_k^s\right)^2 + \left(y_k^s\right)^2}} - \nu_{ke}^s \, g_{kx}^s \,, \tag{13}$$

$$\frac{dg_{ky}^{s}}{dt} = -\frac{q_k \, \left(E\, y_k^s - g_{kz}^s \, B\, y_k^s \right)}{m_k \sqrt{\left(x_k^s\right)^2 + \left(y_k^s\right)^2}} - \nu_{ke}^s \, g_{ky}^s \,, \tag{14}$$

$$\frac{dg_{kz}^{s}}{dt} = -\frac{q_k \, B \, \left(x_k^s \, g_{kx}^s + y_k^s \, g_{ky}^s \right)}{m_k \sqrt{\left(x_k^s\right)^2 + \left(y_k^s\right)^2}} - \nu_{ke}^s \, g_{kz}^s \,. \tag{15}$$

The configuration is energy-momentum conserving.

$$\begin{aligned} g_z &= g_{z0} + \frac{q_k \, B}{m_k} \left(\sqrt{x_0^2 + y_0^2} - \sqrt{x^2 + y^2} \right) \,, \qquad (16) \\ g_x^2 + g_y^2 &= g_{x0}^2 + g_{y0}^2 + \frac{2q_k}{m_k} \left[E - g_{z0} \, B \right] \left(\sqrt{x_0^2 + y_0^2} - \sqrt{x^2 + y^2} \right) - \frac{q_k^2 B^2}{m_k^2} \left(\sqrt{x_0^2 + y_0^2} - \sqrt{x^2 + y^2} \right)^2 \,, \end{aligned}$$

$$g_z = \frac{EB}{B^2} - \sqrt{\left(\frac{EB}{B^2} - g_{z0} \right)^2 + g_{x0}^2 + g_{y0}^2 - g_x^2 - g_y^2} \,.$$

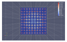

Drift motion of fuel ions

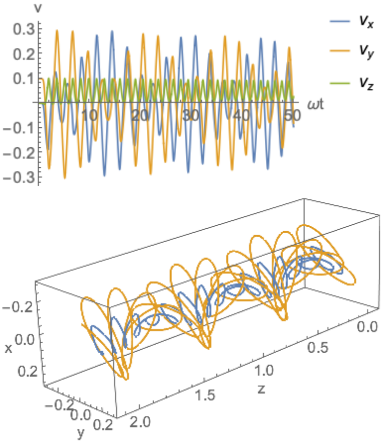

Figure: Gyro motion of fuel ions for $x_0 = 100\ \mu$m, $g_{y0} = 0.1\ c$, $E = 10^{12}$ V/m, $B = 10^4$ vs/m^2, and $\nu_{ke} = 10^{10}$ /s.

The conversion fraction

The cycle-averaged drift field enhanced conversion fraction becomes

$$\eta^{kl} \quad \approx \quad \frac{n_l \, \sigma_0^{kl} \, \sum_s \alpha_k^s \, \int_0^{t_C} dt \, \left|g_k^s(t)\right|_c}{1 + n_l \, \sigma_0^{kl} \, \sum_s \alpha_k^s \, \int_0^{t_C} dt \, \left|g_k^s(t)\right|_c} \, . \tag{17}$$

We have

$$\begin{aligned}
& n_l \sigma_0^{kl} \sum_s \alpha_k^s \int_0^{t_C} dt \, \left|\vec{g}_k^{\,s}(t)\right|_c \\
&= n_l \sigma_0^{kl} \sum_s \alpha_k^s \int_0^{t_C} dt \, \sqrt{a_k \, \left(1 + e^{-2\nu_{ke} t}\right) + b_k^s \, e^{-2\nu_{ke} t}} \\
&= \sigma_0^{kl} \sum_s \alpha_k^s \, \frac{n_l \sqrt{a_k}}{\nu_{ke}} \left[\operatorname{arsinh}\left(\sqrt{\frac{a_k \, e^{2\nu_{ke} t_C}}{a_k + b_k^s}} \right) - \operatorname{arsinh}\left(\sqrt{\frac{a_k}{a_k + b_k^s}} \right) \right] \\
& \quad + \sigma_0^{kl} \sum_s \alpha_k^s \, \frac{n_l \left(\sqrt{2a_k + b_k^s} - \sqrt{\left(a_k + b_k^s\right) \, e^{-2\nu_{ke} t_C} + a_k} \right)}{\nu_{ke}}
\end{aligned} \tag{18}$$

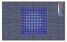

The conversion fraction

under the constraint

$$\sqrt{\frac{2\epsilon_1^{kl}}{m_k}} \leq \sqrt{a_k \, \left(1 + e^{-2\nu_{ke} t}\right) + b_k^s \, e^{-2\nu_{ke} t}} \leq \sqrt{\frac{2\epsilon_2^{kl}}{m_k}} \,, \tag{19}$$

where

$$a_k = \frac{q_k^2 E^2}{m_k^2 \nu_{ke}^2 + q_k^2 B^2} \,, \tag{20}$$

$$b_k^s = \left(\vec{g}_{k0}^{\,s}\right)^2 \,, \tag{21}$$

$$\vec{g}_{k0}^{\,s} = \sqrt{\frac{e_k C_l}{m_k}} \sqrt{R^2 - \left(r_{k0}^s\right)^2} \, \vec{e}_r \,, \tag{22}$$

$$\nu_{ke} \approx \frac{\alpha \, e_k^2 e_e^2 \, n_l \, \ln \Lambda_{ke}}{4\pi \epsilon_0^2 \, m_{ke}^2 \, c^3} \,, \tag{23}$$

$$0 < \alpha < 1 \tag{24}$$

holds for the resistivities and initial velocities. The parameter R is the nano-rod radius, α is the fraction of free electrons, and C_l is the strength of the embedded nano-accelerator composed of the fuel constituent l.

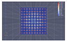

The conversion fraction

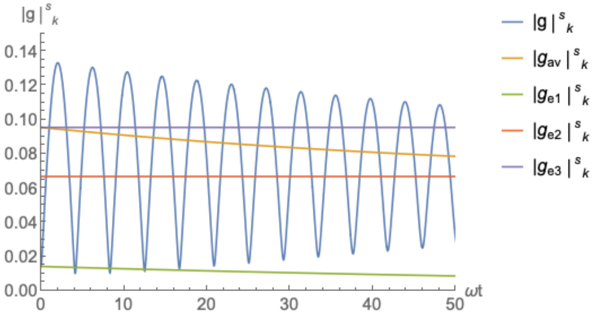

Figure: Illustration of the nonlinear fuel velocity in the drift field configuration denoted by $|g|_k^s$, of the cycle-averaged fuel velocity in the drift field configuration denoted by $|g_{av}|_k^s = \sqrt{a_k \left(1 + e^{-2\nu_{ke}t}\right) + b_k^s\, e^{-2\nu_{ke}t}}$, in the absence of the drift field configuration denoted by $|g_{e1}|_k^s = \sqrt{b_k^s\, e^{-\nu_{ke}t}}$, of $|g_{e2}|_k^s = \sqrt{a_k}$, and of $|g_{e3}|_k^s = \sqrt{2\,a_k + b_k^s}$. The parameters are $\nu_{ke} = 10^{10}\,/\mathrm{s}$, $g_{x0} = 0.01\,c$, $g_{y0} = -0.01\,c$, $g_{z0} = 0.0$, E $= 10^{11}$ V/m, and B $= 10^4$ T. Seeding velocities correspond to the green line.

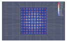

The conversion fraction

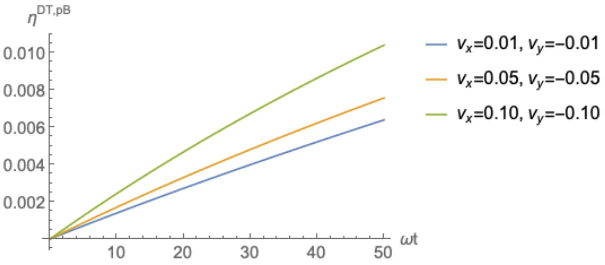

Figure: Conversion fraction $\eta^{DT,pB}$ (with fields plus damping) for various seeding velocities and the limiting cases $\eta_1^{DT,pB}$ (without fields) and $\eta_2^{DT,pB}$ (with fields without damping). The parameters are $E \approx 2.0 \cdot 10^{11}$ V/m, $B \approx 10^4$ Vs/m^2, $\nu_{ke} \approx 10^{10}$ /s. The densities are $n_D = n_T = n_B = n_p = 1.25 \cdot 10^{28}$ m^{-3}.

Literature

H. Ruhl, G. Korn, A laser-driven mixed fuel nuclear fusion reactor concept (Feb. 2022).
doi:10.48550/arXiv.2202.03170.

W. Nevins, R. Swain, The thermonuclear fusion rate coefficient for p-11b reactions, Nuclear fusion 40 (4) (2000) 865.